Topological Percolation on Hyperbolic Simplicial Complexes

Ginestra Bianconi

The Alan Turing Institute, 96 Euston Rd, London NW1 2DB, United Kingdom
School of Mathematical Sciences, Queen Mary University of London, London, E1 4NS, United Kingdom

Robert M. Ziff

Center for the Study of Complex Systems and Department of Chemical Engineering,
University of Michigan, Ann Arbor, Michigan 48109-2136, USA

Simplicial complexes are increasingly used to understand the topology of complex systems as different as brain networks and social interactions. It is therefore of special interest to extend the study of percolation to simplicial complexes. Here we propose a topological theory of percolation for discrete hyperbolic simplicial complexes. Specifically we consider hyperbolic manifolds in dimension $d = 2$ and $d = 3$ formed by simplicial complexes, and we investigate their percolation properties in the presence of topological damage, i.e., when nodes, links, triangles or tetrahedra are randomly removed. We show that in $d = 2$ simplicial complexes there are four topological percolation problems and in $d = 3$, six. We demonstrate the presence of two percolation phase transitions characteristic of hyperbolic spaces for the different variants of topological percolation. While most of the known results on percolation in hyperbolic manifolds are in $d = 2$, here we uncover the rich critical behavior of $d = 3$ hyperbolic manifolds, and show that triangle percolation displays a Berezinskii-Kosterlitz-Thouless (BKT) transition. Finally we provide evidence that topological percolation can display a critical behavior that is unexpected if only node and link percolation are considered.

PACS numbers: 89.75.Fb, 64.60.aq, 05.70.Fh, 64.60.ah

I. INTRODUCTION

Simplicial complexes uncover the topology and geometry of interacting systems such as brain networks [1–3], granular materials [4, 5] and social interaction networks [6]. Simplicial complexes are able to capture higher-order interactions that cannot be encoded in a simple network. In fact they are not just formed by nodes and links but also by higher dimensional simplices such as triangles, tetrahedra and so on.

Simplicial complexes, built by geometrical building blocks, are natural objects to study network geometry [7, 8]. In particular hyperbolic simplicial complexes [9–12] reveal emergent functionalities of complex networks [13] and provide a major avenue to explore the very active area of network hyperbolicity [14–18].

Percolation theory [19–22] studies the properties of the connected components when nodes or links are damaged with probability $q = 1 - p$, fully capturing the network robustness to failure events. However in simplicial complexes, topological damage can be directed not just to nodes and links but also to higher dimensional simplicies. In this respect a major question is how to characterize the robustness of simplicial complexes to topological damage. Given the large variety of systems that can be described by simplicial complexes, this is a challenging theoretical problem of primary importance also for applications. Here we explore the robustness of hyperbolic simplicial complexes by introducing the framework of *topological percolation* and find that the response to damage of higher dimensional simplices can be unexpected if one considers exclusively node or link percolation.

Percolation theory [19–22] of complex networks has been widely studied in the last twenty years. While in uncorrelated random networks percolation is well known to give a single, continuous second-order phase transition in hierarchical networks, it is possible to observe a discontinuous phase transition [23] or a Berezinkii-Kosterlitz-Thouless (BKT) [24, 25] transition [26–28]. Additionally a BKT percolation transition is found also on percolation on growing networks [29–31]. Finally, there is growing interest in investigating generalized percolation problems such as explosive percolation [32–34] and percolation on interdependent multiplex networks [35–38] that have been recently shown to display anomalous critical behavior.

On hyperbolic networks, percolation theory has been shown to display not one but two percolation transitions [39] at the so-called lower p^l and upper p^u percolation thresholds. Below the lower percolation threshold (for $p < p^l$) there is no infinite cluster, above the upper percolation threshold (for $p > p^u$) an extensive infinite cluster exists, and for $p^l < p < p^u$ the average size of the largest cluster is infinite but sub-extensive. Interestingly it has been shown [23], using a renormalization approach, that for hyperbolic $d = 2$ dimensional manifolds called Farey graphs [42, 43] the transition at the upper critical dimension is discontinuous. Several works have studied percolation [26–28, 44–47] and the Ising and Potts models [48, 49] on other hierarchical networks, finding both continuous and discontinous phase transitions. However most of the results on percolation in hyperbolic networks [50, 51] are restricted to $d = 2$ spaces. Here we explore how the scenario change in dimension $d = 3$ and we address the general question whether the nature of the tran-

sition changes with the dimension of the manifold. We consider a class of "holographic" hyperbolic simplicial complexes in $d = 2$ and $d = 3$ that can be extended naturally in higher dimensions. If one only focuses on the nodes and links these simplicial complexes reduce to Farey graphs [42, 43] and to Apollonian networks [52] for dimension $d = 2$ and $d = 3$ respectively.

In order to study the robustness of these simplicial complexes we propose the general framework of topological percolation that includes for each network several percolation problems and is able to capture for each simplicial complex its response to different types of topological damage. Topological percolation expands on previously known types of percolation transitions (node, link and k-clique) percolation. In fact while in node and link percolation random damage is directed either to the nodes or to the links of a network, in topological percolation damage can be directed also to higher-dimensional simplices like triangles, tetrahedra and so on. The topological percolation problems in higher dimensions are very closely connected to k-clique percolation [53, 54] or equivalently (using the topology term) k-connectedness [55] where two k-cliques are considered connected if they share a $(k-1)$-clique. However the topological k-connectedness as well as k-clique percolation have been studied only for non-damaged networks while topological percolation consider the effects of topological damage.

Topological percolation for $d = 2$ simplicial complexes reduces to four percolation problems and for $d = 3$ simplicial complexes reduces to six percolation problems. Topological percolation on the considered hyperbolic simplicial complexes is naturally studied on generalized line graphs which take the form either of single or multiplex networks [35]. Taking advantage of these line graphs here we show that topological percolation in both the $d = 2$ and $d = 3$ dimensional hyperbolic manifolds under consideration displays in general two percolation thresholds (except the trivial case of link percolation on the $d = 3$ hyperbolic manifold). We show however that the nature of the phase transition at the upper percolation threshold can change significantly. In particular our investigation of triangle percolation in the $d = 3$ hyperbolic manifold displays a BKT transition not observed for any of the topological percolation problems in the Farey simplicial complex.

This paper is structured as follows. In Sec. II we define topological percolation on simplicial complexes, in Sec. III we characterize the hyperbolic manifolds under consideration in this work, in Sec. IV we define the general percolation properties of hyperbolic manifolds, in Sec. V we discuss topological percolation in the $d = 2$ hyperbolic manifold, in Sec. V study topological percolation in the $d = 3$ hyperbolic network, in Sec. VI we compare topological percolation for $d = 2$ and $d = 3$ hyperbolic manifolds. Finally in Sec. VII we give the conclusions.

II. TOPOLOGICAL PERCOLATION ON HYPERBOLIC SIMPLICIAL COMPLEXES

Simplicial complexes are not just formed by nodes (0-simplices), and links (1-simplices) but also by higher-dimensional simplices such as triangles (2-simplices), tetrahedra (3-simplices) and so on. Simplicial complexes are the natural objects used in topological data analysis and they are also particularly useful to investigate network geometry because they are formed by geometrical building blocks. Let us now give a more formal definition of simplices and simplicial complexes.

A *simplex* of dimension d (d-simplex) is formed by a set of $d+1$ nodes. The δ-faces of a d-simplex μ are the δ-simplices (with $\delta < d$) that can be constructed by taking a subset of $\delta + 1$ of the nodes of μ. A *simplicial complex* $\mathcal{K}$ of dimension d is formed by a set of δ-dimensional simplices with $\delta \leq d$ glued along their faces (where d is the maximum of all dimensions δ of the simplices belonging to $\mathcal{K}$) with the two properties:

(a) if the simplex μ belongs to the simplicial complex (i.e., $\mu \in \mathcal{K}$) all its faces $\mu' \subset \mu$ also belong to the simplicial complex (i.e., $\mu' \in \mathcal{K}$).

(b) if two simplexes μ, μ' belong to the simplicial complex (i.e., $\mu \in \mathcal{K}$ and $\mu' \in \mathcal{K}$) their intersection is either empty (i.e., $\mu \cap \mu' = \emptyset$) or belongs to the simplicial complex (i.e., $\mu \cap \mu' \in \mathcal{K}$).

Note that the *skeleton* of a simplicial complex is the network formed by its nodes and links.

Simplicial complexes are related to hypergraphs [56]—in fact they can be both considered as sets of sets of nodes. However simplicial complexes satisfy both condition (a) and (b) not satisfied by the hypergraphs. Simplicial complexes are therefore closed under the operation of taking non-empty subsets of each set and this allows for the study of topological properties as a function of the dimensions of its simplices [55].

Here we introduce topological percolation which extends and generalizes node and link percolation to simplicial complexes. In node percolation the properties of the connected components are monitored as a function of the probability $q = 1 - p$ to remove nodes, in link percolation the same properties are studied when links are removed with probability q.

In network science stardard percolation has been leveraged by the notion of k-clique percolation [53, 54] called also by the topologists k-connectedness [55] where cliques of nodes are connected if they share $(k - 1)$-cliques. Therefore k-connected clusters are formed by the sets of k-connected k-cliques. However so far the properties of the k-connected clusters have not been studied in the presence of damage.

Here we consider *topological percolation* that studies the properties of the k-connected clusters [53–55] of the simplicial complexes in presence of *topological damage* that is not only directed to nodes or links but also to higher dimensional simplices.
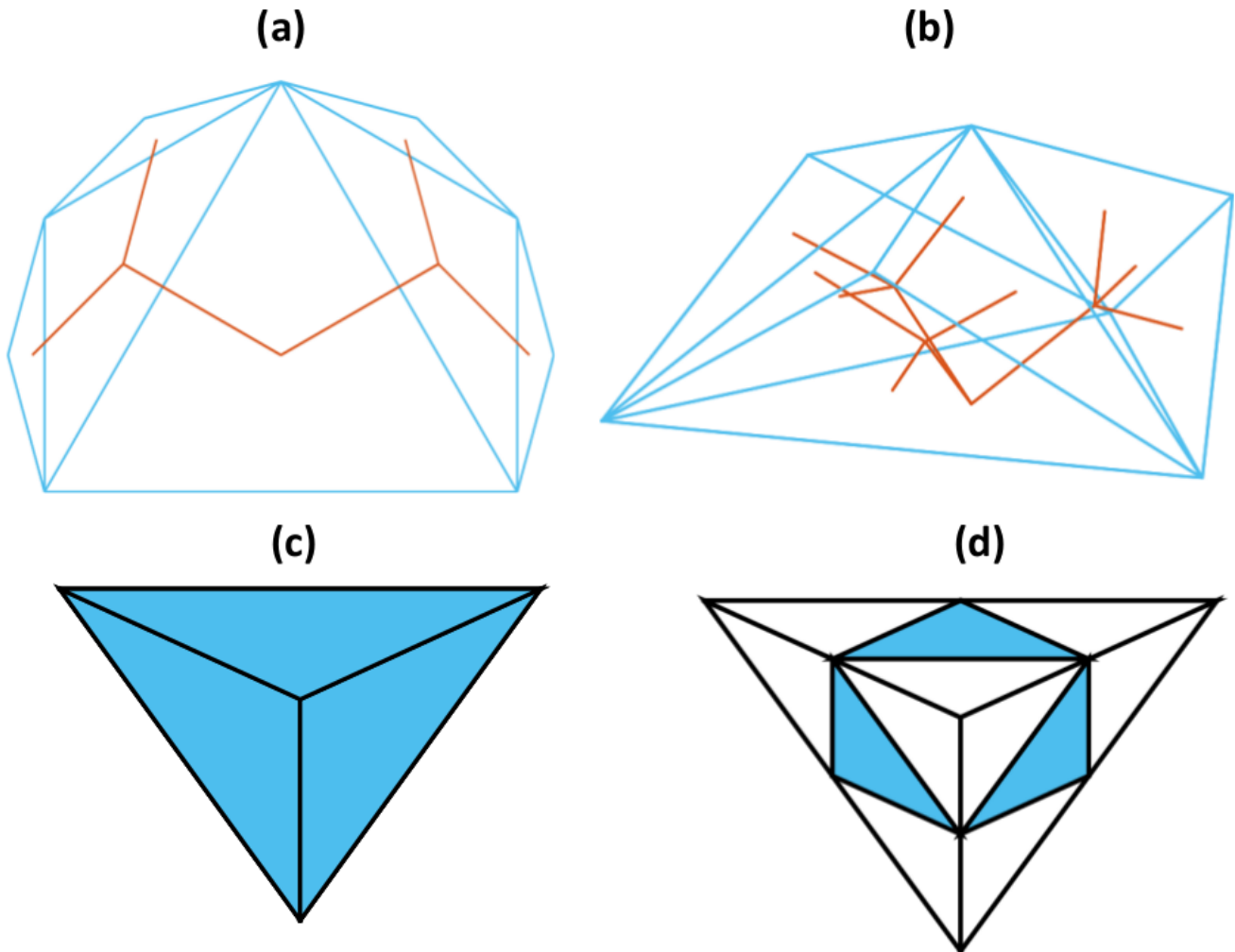
FIG. 1: Panel (a) shows the $d = 2$ skeleton of the Farey simplicial complex at iteration $n = 3$ skeleton (in blue) together with the Cayley tree constituting its generalized line graph (in red). Panel (b) shows the $d = 3$ hyperbolic manifold skeleton (in blue) at iteration $n = 2$ together with the Cayley tree constituting one of its generalized line graphs (in red). Panel (c) shows the Apollonian network at iteration $n = 1$. Panel (d) shows that the Sierpinski gasket simplicial complex (in blue) is a generalized line graph of the Apollonian network (both graphs are shown at iteration $n = 1$).

The choice of the term *topological percolation* is due to the fact that in topology it is usually the case that the properties of a network (or of a graph) are leveraged to the properties of higher dimensional simplices. For instance the graph Laplacian is leveraged to the concept of higher-order Laplacian [57]. Similarly topological percolation includes standard node and link percolation but leverage these two problems also to higher dimensions. Moreover topological percolation characterizes the connectivity of a simplicial complex in presence of topological damage that can produce non-trivial Betti numbers ("holes") in the simplicial complex [58, 59].

In topological percolation we consider percolation among δ-dimensional faces (with $\delta < d$) of the simplicial complex connected through $(\delta + 1)$-faces removed with probability q. For instance in topological percolation in $d = 3$ hyperbolic manifolds includes the distinct percolation problems:

- *Link percolation (also known as bond percolation).* In this case nodes are connected to nodes through links that are removed with probability q.

- *Triangle percolation.* In this case links are connected to links through triangles that are removed with probability q.

- *Tetrahedron percolation.* In this case triangles are connected to triangles through tetrahedra that are removed with probability q.

Moreover topological percolation includes the percolation among δ-dimensional faces (with $0 < \delta < d$) of the simplicial complex connected through $(\delta - 1)$-faces removed with probability q. For simplicial complexes in $d = 3$ therefore topological percolation includes also the distinct percolation problems:
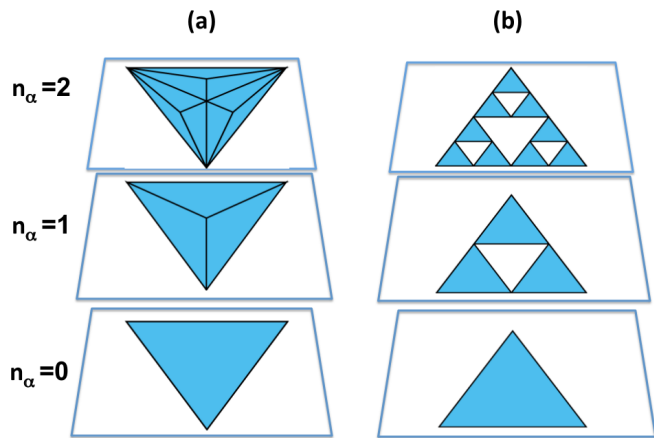
FIG. 2: Panel (a) shows the multiplex network description of the $d = 3$ hyperbolic manifold. Panel (b) show the multiplex Sierpinski gasket that describes a generalized line graph of the $d = 3$ hyperbolic manifold.

- *Node percolation (also known as site percolation).* In this case links are connected to links through nodes that are removed with probability q.

- *Upper-link percolation.* In this case triangles are connected to triangles through links (at the edges of the triangles) that are removed with probability q.

- *Upper-triangle percolation.* In this case tetrahedra are connected to tetrahedra through common triangles that are removed with probability q.

Therefore for $d = 3$ simplicial complexes topological percolation includes six percolation problems. For $d = 2$ simplicial complexes clearly there are only four percolation problems including link percolation, triangle percolation, node percolation and upper-link percolation. In general topological percolation on a d-dimensional simplicial complex includes $2d$ percolation problems.

Note that in node percolation it is customary to indicate that if a node is removed all its links are also removed while for link percolation only the links are removed. This difference is actually redundant if one focuses exclusively on the property of the connectivity of the simplices, as in node percolation a link can be connected to a link only through a node so if we remove that node all the links connected to it will not be part of the percolating cluster automatically. Therefore our definition of the first class of topological percolation problems (including link percolation) is symmetric to the definition of the second set of problems (including node percolation) and there is no need of a distinction between the two cases.

III. HYPERBOLIC NETWORKS UNDER CONSIDERATION

Here we study topological percolation on two classical examples of hyperbolic lattices in dimension $d = 2$ and $d = 3$ and we describe them using simplicial complexes. The first simplicial complex under consideration is the Farey simplicial complex (whose skeleton is the Farey graph [42, 43]). This is an infinite $d = 2$ hyperbolic simplicial complex constructed iteratively starting from a single link (see Fig. 1a). At iteration $n = 1$ we attach a triangle to the initial link. At iteration $n > 1$ we attach a triangle to every link to which we have not yet attached a triangle. The number of nodes $N_n^{(0)}$, links $N_n^{(1)}$ and triangles $N_n^{(2)}$ at iteration n are given by

$$
\begin{aligned}
N_n^{(0)} &= 1 + 2^n, \\
N_n^{(1)} &= 2^{n+1} - 1, \\
N_n^{(2)} &= 2^n - 1.
\end{aligned}
\tag{1}
$$

The second simplicial complex under consideration is the $d = 3$ hyperbolic simplicial complex that generalizes the Farey simplicial complex in dimension $d = 3$. This is an infinite 3-dimensional hyperbolic lattice constructed iteratively starting from a single triangle (see Fig. 1b). At iteration $n = 1$ we attach a tetrahedron to the initial triangle. At iteration $n > 1$ we attach a tetrahedron to each triangle to which we have not yet attached a tetrahedron. The number of nodes $N_n^{(0)}$, links $N_n^{(1)}$, triangles $N_n^{(2)}$ and tetrahedra $N_n^{(3)}$ at iteration n are given by

$$
\begin{aligned}
N_n^{(0)} &= (5 + 3^n)/2, \\
N_n^{(1)} &= (3 + 3^{n+1})/2, \\
N_n^{(2)} &= (3^{n+1} - 1)/2, \\
N_n^{(3)} &= (3^n - 1)/2.
\end{aligned}
\tag{2}
$$

If one focuses exclusively on its skeleton the $d = 3$ hyperbolic simplicial complex we consider in this paper reduces to the Apollonian network [52], so at the network level the two are equivalent. The Apollonian network [52] is a planar network constructed iteratively according to the following algorithm. At iteration $n = 0$ the Apollonian network is formed by a single triangle. At each iteration $n > 1$ each triangle in the $d = 2$ plane is tessellated into three triangles by inserting a node in its center and connecting each of its nodes to the central node (see Fig. 1c). Note however that even though this construction generates the same network skeleton of the $d = 3$ hyperbolic simplicial complex described above, the two models differ if one considers simplices of dimension $d = 2$ (triangles) because in the planar description the triangles are naturally defined exclusively as the faces of the planar representation of the network and they are therefore a subset of the triangles included in the $d = 3$ hyperbolic manifold. Moreover while the $d = 3$ manifold contains tetrahedra, the Apollonian network does not.

Interestingly the Apollonian network is closely related to the Sierpinski gasket [46]. In fact if we construct a network whose nodes correspond to the links of the Apollonian network and two nodes are connected if the corresponding links share a triangle, we obtain the Sierpinski gasket (see Fig. 1d).

We note here that the considered hyperbolic manifolds have "holographic" properties [10–13]. In fact if we define the boundary as the set of all $(d-1)$-faces arrived at the last generation and all their faces, we observe that the considered hyperbolic manifolds in dimension $d = 2$ and dimension $d = 3$ have all the nodes at the boundary. Moreover also all the links are at the boundary therefore at the network level no node or link is lost if we consider the projection of the network on the boundary of the simplicial complex. It follows that the network skeleton of the hyperbolic manifold in dimension $d = 2$ reduces to a hierarchical $d = 1$ network [23] and the one of the hyperbolic manifold in dimension $d = 3$ reduces to the planar ($d = 2$) Apollonian network [52]. This is a perculiar property of these hyperbolic structures shared with the models of emergent geometry in Refs. [9–13] but not shared by other hyperbolic manifolds with a bulk such as the ones studied in Refs. [50, 51].

To uncover the equations for topological percolation in these lattices it is opportune to define a suitable generalization of line graphs to simplicial complexes. A line graph of a network is constructed by placing a node for each link of the original network and connecting these nodes if the corresponding two links are connected by a node in the original network.

Line graphs can be clearly extended to higher dimensions when studying simplicial complexes. For instance in Fig. 1a we show a network whose nodes correspond to the triangles of the Farey simplicial complex and whose links connect nodes corresponding to adjacent triangles in the Farey simplicial complex. Interestingly this network is a Cayley tree of coordination $z = 3$ and will be particularly useful as a reference to study triangle percolation and upper-link percolation on the Farey simplicial complex. For the $d = 3$ hyperbolic network it is possible to construct a Cayley tree of coordination $z = 4$ whose nodes correspond to tetrahedra and links connect nodes corresponding to adjacent tetrahedra (see Fig. 1b). This Cayley graph will be particularly useful to study tetrahedron percolation and upper-triangle percolation. The generalized line graph whose nodes are links of the $d = 3$ hyperbolic manifold and nodes are connected if the corresponding links share a triangle in the original hyperbolic network is a multiplex network with $n+1$ number of layers in which each layer is formed by a Sierpinski gasket (for a definition of multiplex network see Ref. [35]). In order to show this let us observe that the $d = 3$ hyperbolic manifold at iteration n can be described as a multiplex network of $n+1$ layers where each layer $n_\alpha = 0, 1, \ldots, n$ is an Apollonian network at iteration n_α (see Fig. 2a). This construction allows one to take explicitly into account the simultaneous presence of triangles entering the

TABLE I: Lower p^l and upper p^u percolation thresholds for topological percolation on the $d = 2$ and $d = 3$ hyperbolic manifolds under consideration. For each percolation problem the section in which is treated is also indicated.

$d = 2$	section	p^l	p^u
Link percolation	(A1)	0	$\frac{1}{2}$
Triangle percolation	(A2)	$\frac{1}{2}$	1
Node percolation	(A3)	0	1
Upper-link percolation	(A4)	$\frac{1}{2}$	1
$d = 3$	section	p^l	p^u
Link percolation	(B1)	N/A	0
Triangle percolation	(B2)	0	$0.307981\ldots$
Tetrahedron percolation	(B3)	$\frac{1}{3}$	1
Node percolation	(B4)	0	1
Upper-link percolation	(B5)	0	1
Upper-triangle percolation	(B6)	$\frac{1}{3}$	1

$d = 3$ manifold at each iteration. Using the relation between the Apollonian network and the Sierpinski gasket discussed above it is natural to realize that the generalized line graph of this multiplex network whose nodes are the links of the $d = 3$ manifold and two nodes are connected if the corresponding links of the $d = 3$ manifold are incident to the same triangle, can be described as a multiplex Sierpinski gasket of $n + 1$ layers. In this multiplex Sierpinski gasket each layer $n_\alpha = 0, 1, \ldots, n$ is a Sierpinski gasket at iteration n_α (see Fig. 2b). This is the structure on which triangle percolation can be naturally studied.

We note that the different topological percolation problems have very different natures. For instance both link percolation and upper link percolation investigate the effect of damage directed to links; however, while the first one is the traditional link percolation problem the second one studies the 3-connected clusters when links are randomly removed. However all the topological percolation problems can be mapped into node or link percolation in a suitably chosen generalized line graph. For instance upper-link percolation can be recast into a node percolation problem in the generalized line graph in which the links of the original simplicial complex are the nodes and nodes are connected if the corresponding links of the original simplicial complex belong to the same triangle.

IV. GENERAL PROPERTIES OF TOPOLOGICAL PERCOLATION ON THE STUDIED HYPERBOLIC MANIFOLDS

Node and link percolation on hyperbolic manifolds [39] and in general non-amenable graphs [40, 41] are known to have not just one but two percolation thresholds: the lower p^l and the upper p^u percolation thresholds. In particular it is found that the phase diagram of percolation include three regions.

- For $p < p^l$ no cluster has infinite size.

- For $p^l < p < p^u$ the network has an infinite but sub-extensive maximum cluster of average size R

$$R \sim N^{\psi} \qquad (3)$$

with $0 < \psi < 1$. Here N indicates the number of nodes of the network and ψ is called the *fractal critical exponent*.

- For $p > p^u$ the network has an extensive cluster, i.e., the fraction M of nodes in the giant component scales like

$$M \simeq \frac{R}{N} = O(1). \qquad (4)$$

Here we find that these general properties of node and link percolation on hyperbolic lattices remain valid also for the higher-dimensional problems for topological percolation on simplicial complexes (see Table I). However we find that the value of the thresholds, the critical fractal exponent, and the nature of the transition can change significantly for the different versions of the topological percolation and with the overall dimension d of the manifold as will be detailed in the next sections.

V. TOPOLOGICAL PERCOLATION ON $d = 2$ HYPERBOLIC MANIFOLD

In this section we will consider topological percolation on the $d = 2$ Farey simplicial complex in detail. We will summarize known results on link percolation [23] and we will show the critical behavior of node, triangle and upper-triangle percolation.

(A1) Link percolation

In link percolation, links are removed with probability q and the connected component are formed by nodes connected to nodes through intact links. This transition in the $d = 2$ Farey simplicial complex has been studied by Boettcher, Singh and Ziff in Ref. [23].

The probability $\hat{T}_{n+1}$ that the two nodes which appeared in the simplicial complex at iteration $n = 0$ are connected at the generation $n + 1$ is given by [23]

$$\hat{T}_{n+1} = p + (1-p)\hat{T}_n^2. \qquad (5)$$

In fact they are either directly connected (event which occurs with probability p) or if they are not directly connected (event which occurs with probability $q = 1 - p$), they can be connected if each node is connected to the node arrived in the network at iteration $n = 1$ (event which occur with probability $\hat{T}_n^2$). In the limit $n \to \infty$ this equation has the steady-state solution

$$\hat{T}_\infty = \begin{cases} \frac{p}{1-p} & \text{for } p < \frac{1}{2} \\ 1 & \text{for } p \geq \frac{1}{2} \end{cases} .$$

Since we have $\hat{T}_\infty > 0$ for any $p > 0$ and $\hat{T}_\infty = 1$ for $p \geq \frac{1}{2}$, the lower p_1^l and the upper p_1^u critical thresholds are given by

$$p_1^l = 0, \quad p_1^u = \frac{1}{2}. \qquad (6)$$

In order to investigate the nature of the phase transition, Boettcher, Singh and Ziff in Ref. [23] have proposed a theoretical approach based on the generating functions $T_n(x)$ and $S_n(x, y)$. In a Farey simplicial complex at iteration n the function $T_n(x)$ is the generating function of the number of nodes in the connected component linked to both initial nodes. The function $S_n(x, y)$ is the generating function for the sizes of the two connected components linked exclusively to one of the two initial nodes. These generating functions are given by

$$T_n(x) = \sum_{\ell=0}^{\infty} t_n(\ell)x^{\ell},$$
$$S_n(x, y) = \sum_{\ell,\bar{\ell}} s_n(\ell, \bar{\ell})x^{\ell}y^{\bar{\ell}}. \qquad (7)$$

Here we consider the $d = 2$ hyperbolic manifold at iteration n, and we indicate with $t_n(\ell)$ the distribution of the number of nodes ℓ connected to the two initial nodes and with $s_n(\ell, \bar{\ell})$ we indicate the joint distribution of the number of nodes ℓ connected exclusively to a given initial node and the number of nodes $\bar{\ell}$ connected exclusively to the other initial node.

The recursive equations for $T_n(x)$ and $S_n(x, y)$ start from the initial condition $T_0(x) = p$ and $S_0(x, y) = 1 - p$ and read [23]

$$\begin{aligned} T_{n+1}(x) &= p\left\{xT_n^2(x) + 2xT_n(x)S_n(x, x) + S_n(1, x)S_n(1, x)\right\} + (1-p)xT_n^2(x) \\ S_{n+1}(x, y) &= (1-p)\left\{xT_n(x)S_n(x, y) + yS_n(x, y)T_n(y) + S_n(1, x)S_n(1, y)\right\}. \end{aligned} \qquad (8)$$

with

$$\hat{T}_n = T_n(1) = 1 - S_n(1, 1). \qquad (9)$$

The size R_n of the connected component linked to the

initial two nodes at iteration n is given by

$$R_n = \left. \frac{dT_n(x)}{dx} \right|_{x=1}. \tag{10}$$

By explicitly deriving R_n from Eq. (8) in Ref. [23] it has been proven that for $n \gg 1$, R_n scales like

$$R_n \sim [N_n^{(0)}]^\psi \tag{11}$$

with

$$\psi = \frac{1}{\ln 2} \ln \left[\frac{1 + 3p - 4p^2}{2q} + \sqrt{\frac{1 - pq^2}{4q}} \right] \tag{12}$$

where $q = 1 - p$, for $p \leq \frac{1}{2}$. Moreover in Ref. [23] it is also found that

$$M_\infty = \lim_{n \to \infty} \frac{R_n}{N_n^{(0)}} \tag{13}$$

has a discontinuous transition at $p_1^u = \frac{1}{2}$ with $M_\infty^u = 0.609793\ldots$. Interestingly this model is also very closely related to percolation in one-dimensional lattices with long-range links [60, 61].

(A2) Triangle percolation

In triangle percolation, triangles are removed with probability q and the connected components are formed by links that are connected to links through intact triangles. This is node percolation on the Cayley tree network of degree $z = 3$ where nodes are triangles and links connect two adjacent triangles.
We evaluate the percolation properties of this network by measuring the average number of triangles R_n that at iteration n are connected to the triangle added at iteration $n = 1$. At iteration $n = 1$ we have clearly $R_1 = p$. For any $n \geq 1$ R_{n+1} is given by the recursive equation

$$R_{n+1} = p(z - 1)R_n, \tag{14}$$

for arbitrary coordination number z with explicit solution

$$R_n = [p(z - 1)]^{n-1} R_1. \tag{15}$$

Asymptotically, for $n \gg 1$ we R_n scales like

$$R_n \sim [N_n^{(2)}]^\psi, \tag{16}$$

where

$$\psi = \frac{\ln[p(z - 1)]}{\ln 2} = \frac{\ln[2p]}{\ln 2}. \tag{17}$$

for $z = 3$. Therefore there are two percolation transitions at

$$p_2^l = \frac{1}{z - 1} = \frac{1}{2}, \ p_2^u = 1. \tag{18}$$

The lower percolation threshold p_2^l is found by imposing $\psi = 0$ and the upper percolation threshold p_2^u is found by imposing $\psi = 1$. We denote the fraction of triangles in the largest connected component in an infinite Farey simplicial complex as M_∞, defined by

$$M_\infty = \lim_{n \to \infty} \frac{R_n}{N_n^{(2)}}. \tag{19}$$

This order parameter has a discontinuous transition at p_2^u with

$$M_\infty = \begin{cases} 0 & \text{if } p < p_2^u \\ 1 & \text{if } p = p_2^u \end{cases}. \tag{20}$$

(A3) Node percolation

In node percolation nodes are removed with probability q and the connected components are formed by links connected to links through intact nodes.
In order to study this percolation problem we consider a Farey simplicial complex at iteration n and we calculate the average number of nodes $R_n^{[++]}$ and $R_n^{[+-]}$ connected to the initial link given that its end nodes are either both intact (case $[++]$) or one intact and one removed (case $[+-]$). Starting from the initial condition $R_0^{[++]} = R_0^{[+-]} = 0$ the values of $R_n^{[++]}$ and $R_n^{[+-]}$ are found by iteration of the equations,

$$\mathbf{R}_{n+1} = \mathbf{B}\mathbf{R}_n + p\mathbf{1} \tag{21}$$

where

$$\mathbf{R}_n = \begin{pmatrix} R_n^{[++]} \\ R_n^{[+-]} \end{pmatrix}, \quad \mathbf{1} = \begin{pmatrix} 1 \\ 1 \end{pmatrix}. \tag{22}$$

The matrix $\mathbf{B}$ is given by

$$\mathbf{B} = \begin{pmatrix} 2p & 2(1 - p) \\ p & 1 \end{pmatrix} \tag{23}$$

and has maximum eigenvalue

$$\lambda = \frac{1}{2} + p + \frac{1}{2}\sqrt{1 + 4p - 4p^2}. \tag{24}$$

The solution of Eq. (70) is

$$\mathbf{R}_n = p \sum_{r=0}^{n-1} \mathbf{B}^r \mathbf{1} \tag{25}$$

Therefore the leading term for $\mathbf{R}_n$ is

$$\mathbf{R}_n \sim p\lambda^n \sim [N_n^{(0)}]^\psi \tag{26}$$

with

$$\psi = \frac{\ln \lambda}{\ln 2}. \tag{27}$$

By imposing $\psi = 0$ we get p_3^l, and by imposing $\psi = 1$ we get p_3^u, whose numerical values are

$$p_3^l = 0, \ p_3^u = 1. \tag{28}$$

At p_3^u the fraction M_∞ of nodes in the largest component of an infinite Farey simplicial complex, defined as

$$M_\infty = \lim_{n \to \infty} \frac{R_n}{N_n^{(0)}} \tag{29}$$

has a discontinuous jump, i.e.,

$$M_\infty = \begin{cases} 0 & \text{if } p < p_3^u \\ 1 & \text{if } p = p_3^u \end{cases}. \tag{30}$$

(A4) Upper-link percolation

In upper-link percolation links are removed with probability q and one considers the connected components formed by triangles connected to triangles through intact links. This is link percolation on the Cayley tree network of degree $z = 3$ where nodes are triangles and links connect two adjacent triangles.
By indicating with R_n the average number of triangles connected to the initial link at iteration n we have $R_1 = p$ and

$$R_n = p(1 - z)R_{n-1}. \tag{31}$$

These are the same equations found in triangle percolation (15). Therefore we find that the lower and upper percolation thresholds are given by

$$p_4^l = \frac{1}{2}, \ p_4^u = 1 \tag{32}$$

with the same critical behavior found for triangle percolation. Therefore R_n for $n \gg 1$ obeys the scaling in Eq. (16) with the fractal critical exponent ψ given by Eq. (17). Moreover at p_4^u the order parameter M_∞ defined as in Eq. (19) has a discontinuous jump described by

$$M_\infty = \begin{cases} 0 & \text{if } p < p_4^u \\ 1 & \text{if } p = p_4^u \end{cases}. \tag{33}$$

VI. TOPOLOGICAL PERCOLATION ON $d = 3$ HYPERBOLIC MANIFOLD

The characterization of all the topological percolation problems for the $d = 2$ Farey simplicial complex has shown the ubiquitous presence of two percolation transitions typical of hyperbolic networks and a consistent presence of a discontinuous phase transition at $p = p^u$. Here our aim is to explore how this critical behavior extends to the $d = 3$ hyperbolic simplicial complex under consideration. Although the construction of the $d = 3$ manifolds is a obvious extension of the construction of

the $d = 2$ Farey simplicial complex, we need to note that the degree distribution of the Farey graph is exponential while the degree distribution of the Apollonian graph is power-law. Interestingly this major difference of the skeleton of the two simplicial complexes under consideration is responsible for the differences in link percolation between these two structures. In fact in the Apollonian network link percolation [47] has a single continuous percolation threshold $p^u = 0$ with a critical scaling characteristic of scale-free networks. However the other topological percolation problems behave very differently for this $d = 3$ hyperbolic manifold. In particular here we show that all the other five topological percolation problems show the ubiquitous presence of two percolation thresholds. Moreover the nature of the transition at the upper percolation threshold p^u can vary. Particularly interesting is the study of triangle percolation that here is shown to display a continuous BKT percolation transition at the upper percolation threshold p^u. This critical behavior is not observed at the level of node and link percolation. Therefore the response to topological damage can be unpredictable if only node and link percolation are considered.

(B1) Link percolation

Given the equivalence between the skeleton of the $d = 3$ hyperbolic simplicial complex and the Apollonian network, link percolation on the $d = 3$ hyperbolic manifold reduces to link percolation in the Apollonian network. This percolation problem has been studied in Refs. [47] and [46]. This is a particular case in which $p_1^u = 0$ and therefore p_1^l is not defined. The percolation transition at $p = p_1^u$ is continuous [47] and close to this phase transition, for $p \ll 1$ the fraction of nodes R_∞ in the giant component of an infinite network obeys the scaling [47]

$$R_\infty \sim e^{-c/p} \tag{34}$$

where $c > 0$ is a constant. Therefore in this case the fractal critical exponent is $\psi = 1$ for every $p > 0$.

(B2) Triangle percolation

In triangle percolation triangles are removed with probability q and the connected components are formed by links connected to links through intact triangles. For instance the initial three links of the triangle at iteration $n = 0$ can be connected if the initial triangle is not removed or, if it is removed, if they are connected through triangles added at a later iteration (see Fig. 3).
In order to study triangle percolation on the $d = 3$ hyperbolic manifold we consider three variables $\hat{T}_n, \hat{S}_n, \tilde{W}_n$ indicating, at iteration n, the probability that the three
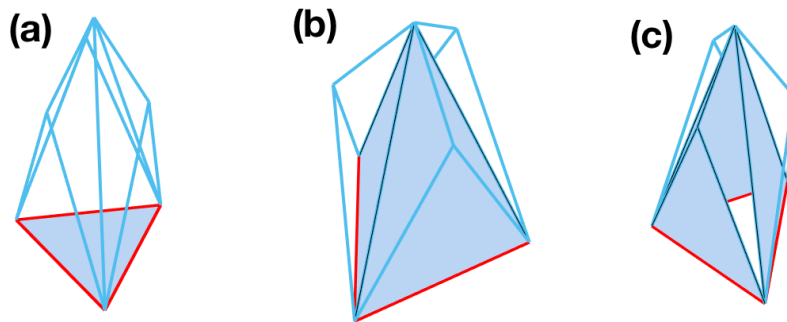
FIG. 3: Examples of how the three initial links of the $d = 3$ hyperbolic manifold (indicated in red) can be connected in triangle percolation: (panel a) through the presence of the initial triangle, (panel b,c) in absence of the initial triangle, through the presence of triangles entered at later iterations.

initial links are connected, that only two of the initial links are connected and that none of the initial links are connected respectively. In terms of the multiplex Apollonian network with $n + 1$ layers (n iterations), $\hat{T}_n$ is the probability that each pair of the three original links is connected (through triangles) in at least in one layer. $\hat{S}_n$ is the probability that two links are connected in at

least one layer (through triangles) and the other link is not connected to the other two in any layer. $\hat{W}_n$ is the probability that no pair of links among the three initial nodes is connected in any layer. The recursive equations for the probabilities $\hat{T}_n, \hat{S}_n$, and $\hat{W}_n$ start from the initial condition $\hat{T}_0 = p$, $\hat{S}_0 = 0$ and $\hat{W}_0 = 1 - p$ and read

$$
\begin{aligned}
\hat{T}_{n+1} &= p + (1-p)(\hat{T}_n^3 + 6\hat{T}_n^2\hat{S}_n + 3\hat{T}_n\hat{S}_n^2), \\
\hat{S}_{n+1} &= (1-p)\left[\hat{T}_n^2(\hat{S}_n + \hat{W}_n) + \hat{T}_n\hat{S}_n(7\hat{S}_n + 2\hat{W}_n) + \hat{S}_n^2(4\hat{S}_n + \hat{W}_n)\right], \\
\hat{W}_{n+1} &= 1 - 3\hat{S}_{n+1} - \hat{T}_{n+1}.
\end{aligned}
\tag{35}
$$

The first equation for $\hat{T}_{n+1}$ indicates that the three links of the original network are connected if the triangle that connects the three links is there in the layer $n_\alpha = 0$ of the multiplex Apollonian network, and if the triangle is not there they must be connected through a chain of triangles in the layers $n_\alpha > 0$. The second equation for $\hat{S}_{n+1}$ indicates that out of the three links of the original network only two are connected by paths passing through triangles. This can occur only if the triangle connecting the three links directly in the layer $n_\alpha = 0$ of the multiplex Apollonian network does not exist and two given links are connected by triangles in the layer $n_\alpha > 0$. Finally the last equation is a normalization condition. By using the vector $\hat{\mathbf{V}}_n = (\hat{T}_n, \hat{S}_n, \hat{W}_n)$, the Eqs. (35) can be written as

$$\hat{\mathbf{V}}_{n+1} = \mathbf{G}(\hat{\mathbf{V}}_n), \tag{36}$$

admitting the asymptotic solution $\hat{\mathbf{V}}_\infty$ for $n \to \infty$ satisfying

$$\hat{\mathbf{V}}_\infty = \mathbf{G}(\hat{\mathbf{V}}_\infty). \tag{37}$$

This equation admits a solution $\hat{T}_\infty > 0$ for every $p > 0$ so the lower critical threshold is $p_2^l = 0$. Moreover

this equation has a singular discontinuity at the point p^u where the maximum eigenvalue Λ_G of the Jacobian of $\mathbf{G}$ satisfies

$$\Lambda_G|_{\hat{\mathbf{V}}=\hat{\mathbf{V}}_\infty} = 1. \tag{38}$$

In fact for $p > p^u$ the only stable solution is $\hat{T}_\infty = 1, \hat{S}_\infty = \hat{W}_\infty = 0$. By imposing Eq. (37) and (38) we get that $p_2^u = 0.307981\ldots$ and $\hat{\mathbf{V}}_\infty^u = (0.509801, 0.0934843, 0.209745)$. Therefore the lower and upper critical thresholds are

$$p_2^l = 0, \; p_2^u = 0.307981\ldots. \tag{39}$$

The emergence of the discontinuity in $\hat{T}_\infty$ can be clearly appreciated from Fig. 7. For details on the numerical calculation see Supplemenary Information [62].

In order to investigate the nature of the upper percolation transition we define the generating functions $T_n(x), S_n(x,y)$ and $W_n(x,y,z)$. These generating func-
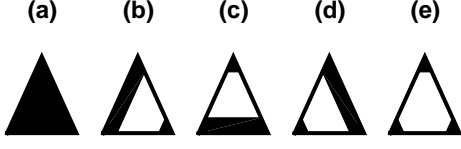
FIG. 4: Schematic diagrams representing $T_n(x)$ (a), $S_n(x,y)$ (b), $S_n(x,z)$ (c), $S_n(y,x)$ (d), and $W_n(x,y,z)$ (e). With x, y and z we indicate the conjugated variables of the components connected with the bottom left, bottom right and top node respectively.

tions are defined as

$$T_n(x) = \sum_{\ell=0}^{\infty} t_n(\ell)x^\ell,$$

$$S_n(x,y) = \sum_{\ell,\bar{\ell}} s_n(\ell,\bar{\ell})x^\ell y^{\bar{\ell}}$$

$$W_n(x,y,z) = \sum_{\ell,\bar{\ell},\hat{\ell}} w_n(\ell,\bar{\ell},\hat{\ell})x^\ell y^{\bar{\ell}} z^{\hat{\ell}}, \qquad (40)$$

with

$$\hat{T}_n = T_n(1), \ \hat{S}_n = 1 - S_n(1,1), \ \hat{W}_n = W_n(1,1,1). \ (41)$$

Given a $d = 3$ hyperbolic manifold at iteration n, $t_n(\ell)$ indicates the distribution of the number of links ℓ connected to the three initial links; $s_n(\ell,\bar{\ell})$ indicates the joint distribution of the number of links ℓ connected to two initial links and the number of links $\bar{\ell}$ connected exclusively to the third initial link; finally $w_n(\ell,\bar{\ell},\hat{\ell})$ indicates the joint distribution of observing $\ell,\bar{\ell},\hat{\ell}$ links connected to each of the initial links. Note that given the definition above $W(x,y,z)$ is left unchanged by a permutation of its variables, while $S_n(x,y)$ is not.

The generating functions $T_n(x), S_n(x,y), W_n(x,y,z)$ can be expressed diagrammatically as shown in Fig. 4. This description is taking advantage of the relation between the multiplex Sierpinski gasket and the $d = 3$ hyperbolic manifold. In particular indicating with x, y, z the conjugated variables to the number of links connected to the initial three links of the $d = 3$ hyperbolic manifolds the panels (a,b,c,d,e) of Fig. 4 represent $T_n(x), S_n(x,y), S_n(x,z), S_n(y,x), W_n(x,y,z)$ respectively. In fact in this aggregated Sierpinski gasket where nodes represent the links of the original aggregated $d = 3$ hyperbolic network, $T_n(x)$ is the generating function of the component connected to the three nodes of the triangle, $S_n(x,y)$ is the generating function of the two separate component connected to two out of thee nodes and to the remaining node respectively, and $W_n(x,y,z)$ is the generating function of the three separate components connected to each node of the aggregated Sierpinski gasket.

For $T_n(x), S_n(x,y)$ and $W_n(x,y,z)$ it is possible to write down recursive equations implementing the renormalization group on these structures (see Appendix).
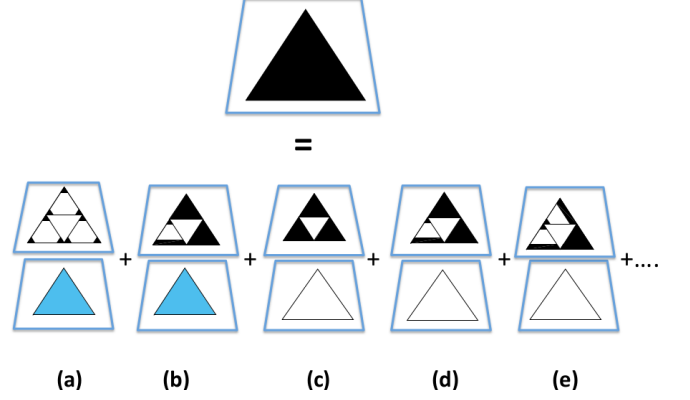

FIG. 5: Diagrammatic expression for some terms of the recursive equation for $T_{n+1}(x)$ given in the Appendix. The different terms indicate $pW_n^3(x,1,1)$ (a), $pT_n^2(x)S_n(x,x)$ (b), $(1-p)T_n^3(x)$ (c), $(1-p)T_n^2(x)S_n(x,x)$ (d), and $(1-p)T_n(x)S_n(x,x)$ (e).
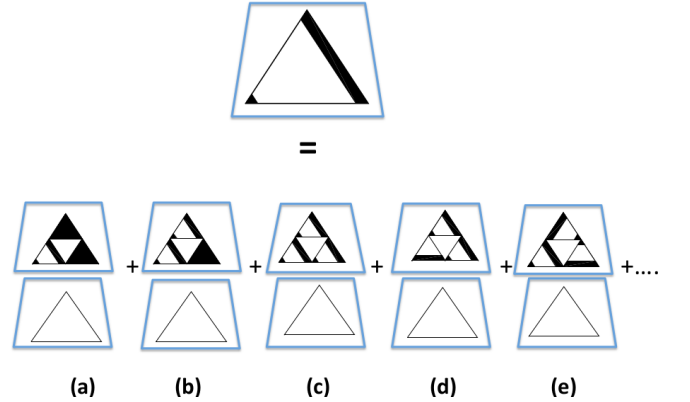

FIG. 6: Diagrammatic expression for the recursive equation for $S_{n+1}(y,x)$. The different terms indicate $(1-p)T_n^2(y)S_n(y,x)$ (a), $(1-p)T_n(y)S_n(y,y)S_n(y,x)$ (b), $(1-p)S_n(1,x)S_n^2(y,1)(x)$ (c), $(1-p)S_n(x,1)S_n(y,1)S_n(y,x)$ (d), and $(1-p)S_n(y,x)S_n^2(y,1)$ (e).

These recursive equations can be written down by using a long but straightforward diagrammatic expansion. In Figs. 5 and 6 we show a few terms of these diagrammatic expression for calculating $T_{n+1}(x)$ and $S_{n+1}(y,x)$. The terms that contribute to $T_{n+1}(x)$ are of two types :

(i) The terms in which the three initial nodes (of the Sierpinski gasket) are directly connected by a triangle at iteration $n = 0$ and in addition they can be connected to other nodes if one takes into account any other iteration (see for instance Fig. 5, panels a, b).

(ii) The terms in which the three initial nodes (of the Sierpinski gasket) are not directly connected by a triangle at iteration $n = 0$ but they are connected if one takes into account any other iteration (see

for instance Fig. 5, panels c, d, e).

The terms that contribute to $S_{n+1}(y, x)$ only include diagrams in which the three initial nodes (of the Sierpinski gasket) are not directly connected (see Fig. 5).

In order to study triangle percolation our first aim is to calculate the average size R_n of the component connected to each one of the three initial links, i.e.,

$$R_n = \frac{dT_n(x)}{dx}\bigg|_{x=1}. \tag{42}$$

and to evaluate the fractal exponent ψ characterizing its asymptotic scaling for $n \gg 1$

$$R_n = [N_n^{(1)}]^\psi. \tag{43}$$

Our second aim is to study the upper percolation transition using the order parameter M_n given by

$$M_n = \frac{R_n}{N_n^{(1)}} \tag{44}$$

in the limit $n \to \infty$.

To this end we note the both goals can be achieved if we characterize $T_n(x)$. From the recursive equations valid for the generating functions, we note that $T_{n+1}(x)$ depends only on the variables $S_n(x, x), S_n(x, 1), S_n(1, x), W_n(x, x, x), W_n(x, x, 1)$ and $W_n(x, 1, 1)$. Therefore $T_n(x)$ can be found by solving a recursive non-linear system of equations for these variables (see Appendix and Supplementary Information [62]). If we define vector $\mathbf{V}_n(x)$ whose components are given by

$$\begin{aligned} V_n^1(x) &= T_n(x), & V_n^2(x) &= S_n(x, x), \\ V_n^3(x) &= S_n(x, 1), & V_n^4(x) &= S_n(1, x), \\ V_n^5(x) &= W_n(x, x, x), & V_n^6(x) &= W_n(x, x, 1), \\ V_n^7(x) &= W_n(x, 1, 1). \end{aligned} \tag{45}$$

this system of equations can be written as a recursive equation for $\mathbf{V}_{n+1}(x)$ given by

$$\mathbf{V}_{n+1}(x) = \mathbf{F}(\mathbf{V}_n(x), x). \tag{46}$$

Finally this system of equations can be differentiated obtaining

$$\frac{d\mathbf{V}_n(x)}{dx} = \sum_{i=1}^{7} \frac{\partial \mathbf{F}(x)}{\partial V_n^i(x)} \frac{dV_n^i(x)}{dx} + \frac{\partial \mathbf{F}(x)}{\partial x}, \tag{47}$$

with initial condition $\mathbf{V}' = (0, 0, 0, 0, 0, 0, 0)$ (the initial nodes are not counted). Since the non-homogeneous term $\partial \mathbf{F}(x)/\partial x$ is subleading with respect to the homogeneous one, for $n \gg 1$

$$\mathbf{V}_n'(x) \propto (\lambda_J)^n \tag{48}$$

with λ_J indicating the maximum eigenvalue of the matrix

$$J_{ij} = \frac{\partial F^i(x)}{\partial V^j(x)}\bigg|_{\mathbf{V}(x)=\mathbf{V}_\infty(1); x=1}. \tag{49}$$

This implies that R_n for $n \gg 1$ scales like

$$R_n \sim [N_n^{(1)}]^\psi \tag{50}$$

with the fractal critical exponent ψ given by

$$\psi = \frac{\ln \lambda_J}{\ln 3}. \tag{51}$$

This fractal critical exponent ψ is plotted in Fig. 7 where one can note its discontinuity at $p = p_2^u$. Finally by evaluating recursively the system of Eqs. (47) we can calculate

$$M_n = \frac{1}{N_n^{(1)}} \frac{dV_n^1(x)}{dx}\bigg|_{x=1}. \tag{52}$$

The dependence of M_n on p is plotted in Fig. 7 for increasing values of n from which we can observe a very sharp but continuous transition at p_2^u. A careful finite size analysis (see [62]) of the critical behavior of M_n for $\Delta p \ll 1$ (see Fig. 8) reveals that the BKT nature of the transition at p_2^u with a critical scaling valid for $\Delta p \ll 1$

$$M_\infty = A e^{-d|\Delta p|^{-\sigma}} \tag{53}$$

with A, d positive constants and $\sigma = 0.50$. This behavior is in agreement with renormalization-group [28] general results on hierarchical networks according to which a hybrid transition in $\hat{T}_\infty$ should result in BKT transition for M_∞. Note the BKT transition has been also observed for percolation [27] and for the Ising model [63, 64] in other hierarchical networks.

(B3) Tetrahedron percolation

In tetrahedron percolation, tetrahedra are removed with probability q and triangles are connected to triangles through intact tetrahedra. This is node percolation on the Cayley tree network of degree $z = 4$ where nodes are tetrahedra and links connect two adjacent tetrahedra along a triangular face. By indicating with R_n the average number of tetrahedra connected to the initial triangle at iteration n we have $R_1 = p$ and

$$R_n = p(1 - z)R_{n-1} \tag{54}$$

(identical to (15) and (31)) with explicit solution

$$R_n = [p(1 - z)]^{n-1}R_1. \tag{55}$$

Therefore, for $n \gg 1$, R_n scales as

$$R_n \simeq [N_n^{(3)}]^\psi \tag{56}$$

where the fractal critical exponent is given by

$$\psi = \frac{\ln[p(z - 1)]}{\ln 3} = \frac{\ln[3p]}{\ln 3}. \tag{57}$$
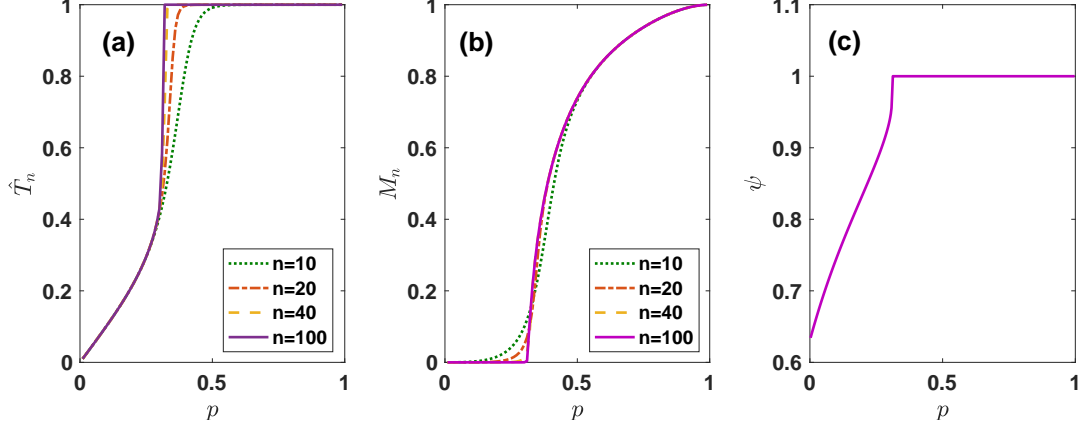
FIG. 7: We plot the statistical mechanics quantities characterizing triangle percolation in the $d = 3$ hyperbolic manifold as a function of p: the probability $\hat{T}_n$ that the three initial links are connected at iteration $n = 10, 20, 40, 100$ (panel a); the fraction M_n of links in the largest component at iterations $n = 10, 20, 40, 100$ (panel b); the fractal critical exponent ψ (panel c).
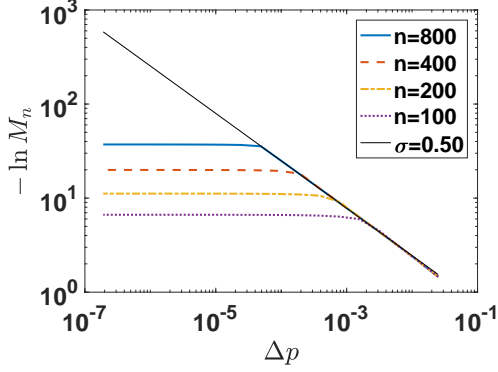

FIG. 8: The BKT critical scaling of M_n versus $\Delta p = p - p_c$ of triangle percolation on the $d = 3$ hyperbolic network for $n = 100, 200, 400, 800$ is plotted together with the theoretical expectation $-\ln M_\infty \simeq -d|\Delta p|^{-\sigma}$ with $\sigma = 0.5$ for $\Delta p \ll 1$.

taking $z = 4$. Therefore we find that the lower and upper percolation thresholds are given by

$$p_3^l = \frac{1}{3}, \; p_4^u = 1. \tag{58}$$

The order parameter M_∞ given by

$$M_\infty = \lim_{n \to \infty} \frac{R_n}{N^{(3)}} \tag{59}$$

and indicating the fraction of tetrahedra in the largest component, has a discontinuous critical behavior, i.e.,

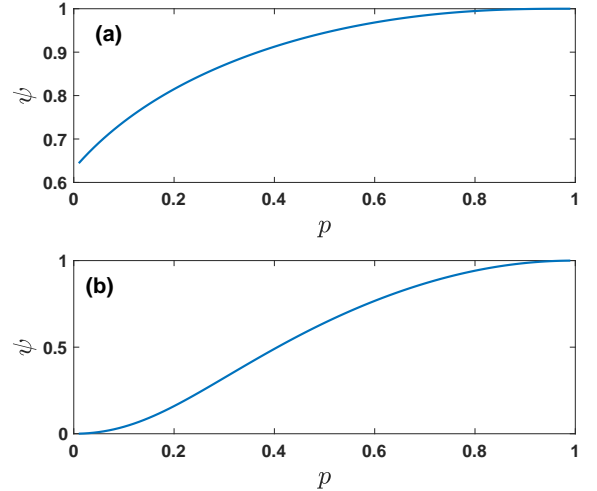$$M_\infty = \begin{cases} 0 & \text{if } p < p_3^u \\ 1 & \text{if } p = p_3^u \end{cases}. \tag{60}$$

FIG. 9: The fractal critical exponent ψ plotted versus p for node percolation (panel a) and upper-link percolation (panel b) on the $d = 3$ hyperbolic manifold.

(B4) Node percolation

In node percolation nodes are removed with probability q and links are connected to links through intact nodes.

In order to study this percolation problem we consider the variables $R_n^{[+++]}$, $R_n^{[++-]}$ and $R_n^{[+--]}$ indicating (at iteration n) the average number of nodes of the component connected to the initial triangle that has three intact nodes, only two intact nodes, or only one intact node, respectively (cases $[+++], [++-], [+--]$). Starting from the initial condition $R_0^{[+++]} = R_0^{[++-]} = R_0^{[+--]} = 0$ the values of $R_n^{[+++]}$, $R_n^{[++-]}$ and $R_n^{[+--]}$ are found by

iteration of the equations,

$$\mathbf{R}_{n+1} = \mathbf{B}\mathbf{R}_n + p\mathbf{1} \tag{61}$$

where

$$\mathbf{R}_n = \begin{pmatrix} R_n^{[+++]} \\ R_n^{[++-]} \\ R_n^{[+--]} \end{pmatrix}, \quad \mathbf{1} = \begin{pmatrix} 1 \\ 1 \\ 1 \end{pmatrix} \tag{62}$$

and

$$\mathbf{B} = \begin{pmatrix} 3p & 3(1-p) & 0 \\ p & 2p+(1-p) & 2(1-p) \\ 0 & 2p & p+2(1-p) \end{pmatrix}. \tag{63}$$

The solution of Eq. (70) is given by

$$\mathbf{R}_n = p\sum_{r=0}^{n-1} \mathbf{B}^r\mathbf{1}. \tag{64}$$

Therefore by indicating with λ the maximum eigenvalue of $\mathbf{B}$, the leading term for $n \gg 1$ goes like

$$\mathbf{R}_n \sim p\lambda^n \sim [N_n^{(0)}]^\psi \tag{65}$$

with

$$\psi = \frac{\ln\lambda}{\ln 3}. \tag{66}$$

In Figure 9a we plot ψ versus p.

By imposing that the maximum eigenvalue $\psi = 1$ we get p_4^u (extensive cluster) and by imposing $\psi = 0$ we get p_4^l. The percolation thresholds are therefore found at

$$p_4^l = 0, \ p_4^u = 1. \tag{67}$$

The order parameter M_∞ given by

$$M_\infty = \lim_{n\to\infty} \frac{R_n}{N^{(0)}} \tag{68}$$

and indicating the fraction of nodes in the largest component, has a discontinuous critical behavior i.e.,

$$M_\infty = \begin{cases} 0 & \text{if } p < p_4^u \\ 1 & \text{if } p = p_4^u \end{cases}. \tag{69}$$

(B5) Upper-link percolation

In upper-link percolation links are removed with probability q and triangles are connected to triangles through intact links.

In order to characterize this topological percolation problem we consider the variables $R_n^{[+++]}$, $R_n^{[++-]}$ and $R_n^{[+--]}$ indicating (at iteration n) the average number of links of the component connected to an intact link of an initial triangle given that the initial triangle has three intact links, only two intact links, or only one intact link

respectively (cases $[+++], [++-], [+--]$). Starting from the initial condition $R_0^{[+++]} = R_0^{[++-]} = R_0^{[+--]} = 0$ the values of $R_n^{[+++]}, R_n^{[++-]}$ and $R_n^{[+--]}$ are found by iteration of the equations,

$$\mathbf{R}_{n+1} = \mathbf{B}\mathbf{R}_n + \mathbf{R}_1 \tag{70}$$

where

$$\mathbf{R}_n = \begin{pmatrix} R_n^{[+++]} \\ R_n^{[++-]} \\ R_n^{[+--]} \end{pmatrix}, \quad \mathbf{R}_1 = (p^3 + 6p^2q + 2pq^2)\begin{pmatrix} 1 \\ 1 \\ 1 \end{pmatrix}$$

and

$$\mathbf{B} = \begin{pmatrix} 3p^3 + 3p^2q & 4p^2q + 6pq^2 & pq^2 + q^3 \\ 2p^3 + 2p^2q & p^3 + 5p^2q + 3pq^2 & 2p^2q + pq^2 + q^3 \\ p^3 + p^2q & 2p^3 + 2p^2q + 2pq^2 & 2p^2q + pq^2 + q^3 \end{pmatrix} \tag{71}$$

where $q = 1 - p$. The solution of Eq. (70) is given by

$$\mathbf{R}_n = \sum_{r=0}^{n-1} \mathbf{B}^r\mathbf{R}_1. \tag{72}$$

Therefore by indicating with λ the maximum eigenvalue of $\mathbf{B}$ given by Eq. (71), the leading term for $n \gg 1$ goes like

$$\mathbf{R}_n \sim p\lambda^n \sim [N_n^{(1)}]^\psi \tag{73}$$

with

$$\psi = \frac{\ln\lambda}{\ln 3}. \tag{74}$$

The numerically evaluated the fractal exponent ψ is plotted versus p in Fig. 9b. By imposing $\psi = 0$ we get p_5^l, by imposing $\psi = 1$ we get p_5^u. The percolation threshold are therefore found at

$$p_5^l = 0, \ p_5^u = 1. \tag{75}$$

The order parameter M_∞ is given by

$$M_\infty = \lim_{n\to\infty} \frac{R_n}{N^{(1)}} \tag{76}$$

and indicating the fraction of links in the largest component has a discontinuous critical behavior, i.e.,

$$M_\infty = \begin{cases} 0 & \text{if } p < p_5^u \\ 1 & \text{if } p = p_5^u \end{cases}. \tag{77}$$

$$\tag{78}$$

(B6) Upper-triangle percolation

In upper-triangle percolation triangles are removed with probability q and tetrahedra are connected to tetrahedra through intact triangles. This is link percolation

on the Cayley tree network of degree $z = 4$ where nodes are triangles and links connect two adjacent triangles. By indicating with R_n the average number of tetrahedra connected to the initial triangle at iteration n we have $R_1 = p$ and for $n > 1$ we have

$$R_n = p(1 - z)R_{n-1}. \tag{79}$$

These are the same equations found in tetrahedron (54) percolation. Therefore by taking $z = 4$, we find that the lower and upper percolation thresholds are given

$$p_6^l = \frac{1}{3}, \ p_6^u = 1 \tag{80}$$

with the same critical behavior found for tetrahedron percolation. Therefore R_n for $n \gg 1$ obeys the scaling in Eq. (56) with the fractal critical exponent ψ given by Eq. (57). Moreover at p_6^u the order parameter M_∞ defined as in Eq. (59) has a discontinuous jump described by

$$M_\infty \ = \ \begin{cases} 0 & \text{if } p < p_6^u \\ 1 & \text{if } p = p_6^u \end{cases}. \tag{81}$$

$$\tag{82}$$

VII.   COMPARISON BETWEEN TOPOLOGICAL PERCOLATION IN $d = 2$ AND $d = 3$ HYPERBOLIC SIMPLICIAL COMPLEXES

Our detailed study of topological percolation in the $d = 2$ and $d = 3$ hyperbolic simplicial complexes (performed in Secs. V and VI) can be summarized by considering the following major points.

Topological percolation of the $d = 2$ hyperbolic manifold displays the following major properties:

- All topological percolation problems have two percolation thresholds p^l and p^u (given in Table I).

- All topological percolation problems are discontinuous at the upper critical percolation threshold p^u. However with the exception of the non-trivial link percolation problem (A1) studied in Ref. [23] the upper critical percolation threshold is $p^u = 1$ and the discontinuity takes the form of a trivial $0-1$ law for the order parameter M_∞ (see Eqs. (20), (30) and 33).

Topological percolation of the $d = 3$ hyperbolic manifold displays the following major properties:

- All topological percolation problems have two percolation thresholds p^l and p^u (given in Table I) except link percolation (B1) studied in Ref. [47] for which $p^u = 0$ and p^l cannot be defined.

- All topological percolation problems with the exception of link percolation (B1) and triangle percolation (B2) are discontinuous at the upper critical percolation threshold $p^u = 1$ obeying the trivial $0-1$ law (see Eqs. (60), (69), (78) and 82).

- Link percolation (B1) studied in Ref. [47] is continuous at the upper percolation threshold $p^u = 0$ with an exponential critical behavior (see Eqs. 34) typical of scale-free networks.

- Triangle percolation (B2) is continuous at the upper percolation threshold p^u. Moreover it follows an anomalous critical behavior displaying a BKT transition (see Eqs. 53). We observe that the BKT transition is not seen for any other topological percolation problem in the same manifold or in the $d = 2$ hyperbolic manifold.

- In topological percolation on the $d = 3$ hyperbolic manifold not even one topological percolation problem displays a non-trivial discontinuity, i.e., there is no percolation problem with a critical behavior similar to link percolation (A1) in the $d = 2$ hyperbolic manifold.

VIII.   CONCLUSIONS

In this paper we have proposed topological percolation which extends the study of percolation beyond node and link (site and bond) percolation for simplicial complexes. Topological percolation on a d-dimensional simplex refers to a set of $2d$ percolation processes that reveal different topological properties of the simplicial complex. As such this approach can be used on any arbitrary simplicial complex dataset and has relevance for the wide variety of applications where simplicial complexes are used from brain research to social networks. Here we have treated topological percolation on two major examples of $d = 2$ and $d = 3$ hyperbolic simplicial complexes describing discrete manifolds. The $d = 2$ hyperbolic manifold is the Farey simplicial complex, the $d = 3$ hyperbolic simplicial complex has a skeleton given by the Apollonian graph. We have emphasized the ubiquitous presence of two percolation thresholds characteristic of hyperbolic discrete structures for each topological percolation problem with the exception of the trivial link percolation for the $d = 3$ manifold (see Table I). However we have observed that the nature of the phase transitions can vary and that topological percolation reveals properties that are unexpected if one just focuses on the robustness of the network skeleton. In particular here we show that triangle percolation in the $d = 3$ hyperbolic manifold displays a BKT transition while no similar critical behavior is observed at the level of link percolation on the same simplicial complex. Moreover we observe an important dependence of topological percolation with the dimension of the simplicial complex. In fact while the $d = 2$ Farey simplicial complex and the $d = 3$ hyperbolic manifold considered here obey similar generation rules, the BKT transition is only observed in topological percolation of the $d = 3$ manifold. Additionally the peculiar properties of the non-trivial discontinuous link percolation on $d = 2$

hyperbolic manifold are not observed for any of the six topological percolation problems in the $d = 3$ manifold.

In conclusion our work constitutes one of the few studies of percolation on hyperbolic manifolds of dimension $d = 3$ and shows the rich unexpected behavior of topological percolation in higher-dimensional simplicial complexes.

This work can be extended in different directions. The analytical investigation of topological percolation can be extended to hyperbolic cell complexes and higher-dimensional hyperbolic simplicial complexes. Moreover topological percolation can be explored on the increasing number of available simplicial complex datasets such

a collaboration networks, social networks or protein interaction networks which include an important interplay between randomness and order.

Acknowledgements

[1] C. Giusti, R. Ghrist and D. S. Bassett, *Two's company, three (or more) is a simplex,* J. Comp. Neuroscience, **41**, 1 (2016).

[2] G. Petri, P. Expert, F. Turkheimer, R. Carhart-Harris, D. Nutt, P. J. Hellyer, and F. Vaccarino, *Homological scaffolds of brain functional networks,* J. R. Soc. Interface **11**, 20140873 (2014).

[3] M. W. Reimann, M. Nolte, M. Scolamiero, et al., *Cliques of neurons bound into cavities provide a missing link between structure and function,* Front. Comp. Neuro. **11**, 48 (2017).

[4] L. Papadopoulos, L. M. A. Porter, K. E. Daniels, and D. S. Bassett, *Network analysis of particles and grains,* J. Comp. Net. **6**, 485 (2018).

[5] M. Šuvakov, M. Andjelković, and B. Tadić, *Hidden geometries in networks arising from cooperative self-assembly,* Sci. Rep. **8**, 1987 (2018).

[6] G. Petri and A. Barrat, *Simplicial Activity Driven Model*, preprint arXiv:1805.06740 (2018).

[7] Z. Wu, G. Menichetti, C. Rahmede and G. Bianconi, *Emergent complex network geometry,* Sci. Rep. **5**, 10073 (2014).

[8] D. C. da Silva, G. Bianconi, R. A. da Costa, S. N. Dorogovtsev, and J. F. F. Mendes, *Complex network view of evolving manifolds,* Phys. Rev. E **97**, 032316 (2018).

[9] G. Bianconi and C. Rahmede, *Complex quantum network manifolds in dimension $d > 2$ are scale-free,* Sci. Rep. **5**, 13979 (2015).

[10] G. Bianconi and C. Rahmede, *Network geometry with flavor: from complexity to quantum geometry*, Phys. Rev. E **93**, 032315 (2016).

[11] G. Bianconi and C. Rahmede, *Emergent hyperbolic network geometry*, Sci. Rep. **7** 41974 (2017).

[12] D. Mulder and G. Bianconi, *Network Geometry and Complexity* J. Stat. Phys. (2018).

[13] A. P. Millán, J. J. Torres and G. Bianconi, *Complex Network Geometry and Frustrated Synchronization,* Sci. Rep. **8**, 9910 (2018).

[14] R. Kleinberg, *Geographic routing using hyperbolic space* In INFOCOM 2007. 26th IEEE International Conference on Computer Communications. IEEE, 1902, (2007).

[15] M. Boguñá, F. Papadopoulos, and D. Krioukov, *Sustaining the internet with hyperbolic mapping,* Nature Commun. **1**, 62 (2010).

[16] D. Krioukov, F. Papadopoulos, M. Kitsak, A. Vahdat,

and M. Boguñá., *Hyperbolic geometry of complex networks,* Phys. Rev. E **82**, 036106 (2010).

[17] C. C. Ni, Y.-Y. Lin, J. Gao, X. D. Gu, and E. Saucan, *Ricci curvature of the Internet topology* In Computer Communications (INFOCOM), 2015 IEEE Conference on, 2758-2766. IEEE, (2015).

[18] R. Albert, B. DasGupta and N. Mobasheri, *Topological implications of negative curvature for biological and social networks* Phys. Rev. E **89**, 032811 (2014).

[19] S. N. Dorogovtsev and J. F. F. Mendes, *Evolution of networks,* Advances in Physics **51,** 1079 (2002).

[20] S. N. Dorogovtsev, A. V. Goltsev and J. F. F. Mendes, *Critical phenomena in complex networks,* Rev. Mod. Phys. **80**, 1275 (2008).

[21] N. P. Araújo, P. Grassberger, B. Kahng, K. J. Schrenk, and R. M. Ziff, *Recent advances and open challenges in percolation,* Eur. Phys. Jour. Special Topics **223**, 2307 (2014).

[22] D. Lee, Y. S. Cho, K.-I. Goh, D.-S. Lee, B. Kahng, *Recent advances of percolation theory in complex networks,* Jour. Kor. Phys. Soc. **73** 152 (2018).

[23] S. Boettcher, V. Singh, and R. M. Ziff, *Ordinary percolation with discontinuous transitions,* Nature Comm. **3** 787 (2012).

[24] V. L. Berezinskii, *Destruction of long-range order in one-dimensional and two-dimensional systems having a continuous symmetry group I. Classical systems,* Sov. Phys. JETP **32**, 493 (1971).

[25] J. M. Kosterlitz and D. J. Thouless. *Ordering, metastability and phase transitions in two-dimensional systems,* J. Phys. C: Solid State Physics **6**, 1181 (1973).

[26] T. Hasegawa, M. Sato and K. Nemoto, Generating-function approach for bond percolation in hierarchical networks, Phys. Rev. E **82**, 046101 (2010).

[27] T. Nogawa and T. Hasegawa, *Transition-type change between an inverted Berezinskii-Kosterlitz-Thouless transition and an abrupt transition in bond percolation on a random hierarchical small-world network,* Phys. Rev. E **89**, 042803 (2014).

[28] S. Boettcher and C. T. Brunson, *Classification of critical phenomena in hierarchical small-world networks* EPL (Europhysics Letters) **110**, 26005 (2015).

[29] S. N. Dorogovtsev, J. F. F. Mendes, and A. N. Samukhin, *Anomalous percolation properties of growing networks* Phys. Rev. E **64**, 066110 (2001).

[30] D. S. Callaway, J. E. Hopcroft, J. M. Kleinberg, M. E. J. Newman, and S. H. Strogatz, *Are randomly grown graphs really random?*, Phys. Rev. E **64**, 041902 (2001).

[31] S. M. Oh, S-W. Son, and B. Kahng, *Suppression effect on the Berezinskii-Kosterlitz-Thouless transition in growing networks,* preprint arXiv:1805.04442 (2018).

[32] D. Achlioptas, R. M. D'Souza, and J. Spencer, *Explosive percolation in random networks,* Science **323**, 1453 (2009).

[33] R. M. Ziff, *Scaling behavior of explosive percolation on the square lattice,* Phys. Rev. E **82**, 051105 (2010).

[34] R. A. da Costa, S. N. Dorogovtsev, A. V. Goltsev and J. F. F. Mendes, *Explosive percolation transition is actually continuous,* Phys. Rev. Lett. **105**, 255701 (2010).

[35] G. Bianconi, *Multilayer Networks: Structure and Function* (Oxford University Press, Oxford, 2018).

[36] S. V. Buldyrev, R. Parshani, G. Paul, H. E. Stanley and S. Havlin, *Catastrophic cascade of failures in interdependent networks,* Nature **464**, 1025 (2010).

[37] S. W. Son, G. Bizhani, C. Christensen, P. Grassberger, and M. Paczuski, *Percolation theory on interdependent networks based on epidemic spreading,* EPL (Europhysics Letters), **97**, 16006 (2012).

[38] G. J. Baxter, S. N. Dorogovtsev, A. V. Goltsev and J. F. F. Mendes, Avalanche collapse of interdependent networks, Phys. Rev. Lett. **109**, 248701 (2012).

[39] I. Benjamini, and O. Schramm, *Percolation in the hyperbolic plane*, Jour. Am. Math. Soc. **14**,487 (2001).

[40] R. Lyons, *Phase transitions on nonamenable graphs*, Journal of Mathematical Physics, **41**, 1099 (2000).

[41] T. Nogawa, and T. Hasegawa, *Monte Carlo simulation study of the two-stage percolation transition in enhanced binary trees*, Jour. Phys. A **42**, 145001 (2009).

[42] C. J. Colbourn, *Farey series and maximal outerplanar graphs,* SIAM Jour. Alg. Dis. Met. **3**, 187 (1982).

[43] Z. Zhang and F. Comellas, *Farey graphs as models for complex networks*, preprint arXiv:1105.0575 (2011).

[44] S. Boettcher, J. L. Cook and R. M. Ziff, *Patchy percolation on a hierarchical network with small-world bonds*, Phys. Rev. E **80**, 041115 (2009).

[45] V. Singh and S. Boettcher, *Scaling of clusters near discontinuous percolation transitions in hyperbolic networks,* Phys. Rev. E **90**, 012117 (2014).

[46] R. M. Ziff, *Universal behavior of Sierpinski gaskets in the scaling limit* (private communication).

[47] D. M. Auto, A. A. Moreira, H. J. Herrmann and J. S. Andrade Jr., *Finite-size effects for percolation on Apollonian networks,* Phys. Rev. E **78**, 066112 (2008).

[48] S. Boettcher and C. T. Brunson, *Fixed-point properties of the Ising ferromagnet on the Hanoi networks,* Phys. Rev. E **83**, 021103 (2011).

[49] V. Singh, C. T. Brunson and S. Boettcher, *From explosive to infinite-order transitions on a hyperbolic network*, Phys. Rev. E **90**, 052119 (2014).

[50] H. Gu and R. M. Ziff, *Crossing on hyperbolic manifolds*, Phys. Rev. E **85**, 051141 (2012).

[51] S. Mertens and C. Moore, *Percolation thresholds in hyperbolic manifolds*, Phys. Rev. E **96**, 042116 (2017).

[52] J. S. Andrade Jr., H. J. Herrmann, R. F. S. Andrade and L. R. Da Silva, *Apollonian networks: Simultaneously scale-free, small world, Euclidean, space filling, and with matching graphs.* Phys. Rev. Lett. **94**, 018702 (2005).

[53] G. Palla, I. Derényi, I. Farkas, and T. Vicsek, *Uncovering the overlapping community structure of complex networks in nature and society*, Nature **435**, 814 (2005).

[54] I. Derényi, G. Palla, and T. Vicsek, *Clique percolation in random networks*, Phys. Rev. Lett. **94**, 160202 (2005).

[55] M. Kahle,*Topology of random simplicial complexes: a survey,* AMS Contemp. Math, **620** 201 (2014).

[56] G. Ghoshal, V. Zlatić, G. Caldarelli and M. E. J. Newman, *Random hypergraphs and their applications,* Phys. Rev. E, **79**, 066118 (2009).

[57] D. Horak and J. Jost, *Spectra of combinatorial Laplace operators on simplicial complexes. Advances in Mathematics,* **244**, 303 (2013).

[58] G. Bianconi, *Interdisciplinary and physics challenges of network theory,* EPL (Europhysics Letters), **111**, 56001 (2015).

[59] V. Salnikov, D. Cassese and R. Lambiotte, *Simplicial complexes and complex systems*, arXiv preprint arXiv:1807.07747 (2018).

[60] M. Aizenman and C. M. Newman, *Discontinuity of the percolation density in one dimensional $1/|xy|^2$ percolation models.* Comm. Math. Phys., **107**, 611 (1986).

[61] M. Aizenman, J.T. Chayes, L. Chayes, and C. M. Newman, *Discontinuity of the magnetization in one-dimensional $1/|xy|^2$ Ising and Potts models.* Jour. of Stat. Phys., **50**, 1 (1988).

[62] The Supplementary Information is a complete Mathematica notebook on triangle percolation. It is available at xxxx.

[63] E. Khajeh, S. N. Dorogovtsev and J. F. F. Mendes, *Berezinskii-Kosterlitz-Thouless-like transition in the Potts model on an inhomogeneous annealed network,* Phys. Rev. E **75**, 041112 (2007).

[64] M. Hinczewski and A. N. Berker, *Inverted Berezinskii-Kosterlitz-Thouless singularity and high-temperature algebraic order in an Ising model on a scale-free hierarchical-manifold small-world network,* Phys. Rev. E **73**, 066126 (2006).

Appendix: (B2) $d=3$ generating functions

In this appendix we write the recursive equations for the generating functions solving triangle percolation in the $d=3$ hyperbolic manifold and we write explicitly the Eqs. (46). Using the diagrammatic expansion discussed in the main text it is possible to derive the following recursive equations for the generating functions. Starting from the initial condition $T_0(x)=p$, $S_0(x,y)=0$ and $W_0(x,y,z)=1-p$ (the initial nodes are not counted) the recursive equations for $T_n(x), S_n(x,y)$ and $W_n(x,y,z)$ read

$$
\begin{aligned}
T_{n+1}(x) =\ & p\left\{x^3T_n^3(x)+9x^2T_n^2(x)S_n(x,x)+3x^3T_n^2(x)W(x,x,x)+24x^3T_n(x)S_n^2(x,x)+3x^2T_n(x)S_n^2(x,1)\right.\\
&+12x^3T_n(x)S_n(x,x)W_n(x,x,x)+6x^2T_n(x)S_n(x,1)W_n(x,x,1)+3x^2T_n(x)W_n^2(x,x,1)\\
&+14x^3S_n^3(x,x)+9x^2S_n(x,x)S_n^2(x,1)+S_n^3(1,x)\\
&+3xS_n^2(x,1)S_n(1,x)+3S_n^2(1,x)W_n(x,1,1)+6xS_n(x,1)S_n(1,x)W_n(x,x,1)\\
&+12x^2S_n(x,1)S_n(x,x)W_n(x,x,1)+3xS_n^2(x,1)W(x,1,1)\\
&\left.+3x^2S_n^2(x,1)W(x,x,x)+3S_n(1,x)W_n^2(x,1,1)+6S_n(x,1)W_n(x,1,1)W_n(x,x,1)+W_n^3(x,1,1)\right\}\\
&+(1-p)\left\{x^3T_n^3(x)+6x^3T_n^2(x)S(x,x)+3x^2T_n(x)S_n^2(x,1)\right\}\\
S_{n+1}(x,y) =\ & (1-p)\left\{x^3T_n^2(x)S_n(x,y)+x^3T_n^2(x)W_n(x,x,y)+4x^3T_n(x)S_n(x,x)S_n(x,y)\right.\\
&+2x^2yT_n(x)S_n(y,x)S_n(x,y)+2x^2T_n(x)S_n(x,1)W_n(x,y,1)+xy^2T_n(y)S_n^2(x,y)\\
&\left.+xS_n^2(x,1)S_n(1,y)+2xyS_n(x,1)S_n(x,y)S_n(y,1)+xS_n^2(x,1)W_n(y,1,1)+x^2S_n^2(x,1)S_n(x,y)\right\}\\
W_{n+1}(x,y,z) =\ & (1-p)\left\{x^3T_n(x)S_n(x,y)S_n(x,z)+x^3T_n(x)S_n(x,z)W_n(x,x,y)+x^2zT_n(x)S_n(z,x)W_n(x,y,z)\right.\\
&+x^3T_n(x)S_n(x,y)W_n(x,x,z)+x^2yT_n(x)S_n(y,x)W_n(x,y,z)+x^2T_n(x)W_n(x,y,1)W_n(x,z,1)\\
&+z^3T_n(z)S_n(z,x)S_n(z,y)+z^3T_n(z)S_n(z,x)W_n(y,z,z)+xz^2T_n(z)S_n(x,z)W_n(x,y,z)\\
&+z^3T_n(z)S_n(z,y)W_n(x,z,z)+yz^2T_n(z)S_n(y,z)W_n(x,y,z)+z^2T_n(z)W_n(x,z,1)W_n(y,z,1)\\
&+y^3T_n(y)S_n(y,x)S_n(y,z)+y^3T_n(y)S_n(y,x)W_n(y,y,z)+xy^2T_n(y)S_n(x,y)W_n(x,y,z)\\
&+y^3T_n(y)S_n(y,z)W_n(x,y,y)+y^2zT_n(y)S_n(z,y)W_n(x,y,z)+y^2T_n(y)W_n(x,y,1)W_n(z,y,1)\\
&+S_n(1,x)S_n(1,y)S_n(1,z)+2y^3S_n(y,x)S_n(y,y)S_n(y,z)+S_n(1,x)S_n(1,z)W_n(y,1,1)\\
&+z^3S_n(z,x)S_n(z,z)S_n(z,y)+yz^2S_n(z,x)S_n(z,y)S_n(y,z)+z^2S_n(z,x)S_n(z,1)W_n(y,z,1)\\
&+z^3S_n(z,x)S_n(z,z)S_n(z,y)+y^2zS_n(y,x)S_n(z,y)S_n(y,z)+zS_n(1,x)S_n(z,1)W_n(y,z,1)\\
&+S_n(1,x)S_n(1,y)W_n(z,1,1)+yS_n(1,x)S_n(y,1)W_n(y,z,1)+y^2S_n(y,x)S_n(y,1)W_n(y,z,1)\\
&+S_n(1,x)W_n(y,1,1)W_n(z,1,1)+x^3S_n(x,x)S_n(x,z)S_n(x,y)+x^2yS_n(x,y)S_n(y,x)S_n(x,z)\\
&+x^2S_n(x,1)S_n(x,z)W_n(x,y,1)+xz^2S_n(x,z)S_n(z,x)S_n(z,y)+xyzS_n(x,y)S_n(z,x)S_n(y,z)\\
&+xzS_n(x,1)S_n(z,x)W_n(y,z,1)+xS_n(x,1)S_n(1,y)W_n(x,z,1)+xyS_n(x,1)S_n(y,1)W_n(x,y,z)\\
&+xyS_n(x,y)S_n(y,1)W_n(x,z,1)+xS_n(x,1)W_n(x,z,1)W_n(y,1,1)\\
&+x^3S_n(x,x)S_n(x,y)S_n(x,z)+xy^2S_n(x,y)S_n(y,x)S_n(y,z)+xS_n(x,1)S_n(1,z)W_n(x,y,1)\\
&+x^2zS_n(x,z)S_n(x,y)S_n(z,x)+xyzS_n(x,z)S_n(y,x)S_n(z,y)+xzS_n(x,z)S_n(z,1)W_n(x,y,1)\\
&+xzS_n(x,1)S_n(z,1)W_n(x,y,z)+x^2S_n(x,1)S_n(x,y)W_n(x,z,1)+xyS_n(x,1)S_n(y,x)W_n(y,z,1)\\
&+xS_n(x,1)W_n(x,y,1)W_n(z,1,1)\\
&+S_n(1,y)S_n(1,z)W_n(x,1,1)+y^2S_n(y,z)S_n(y,1)W_n(x,y,1)+yS_n(y,1)S_n(1,z)W_n(x,y,1)\\
&+S_n(1,z)W_n(x,1,1)W_n(y,1,1)+zS_n(1,y)S_n(z,1)W_n(x,z,1)+yzS_n(z,y)S_n(y,1)W_n(x,z,1)\\
&+yzS_n(z,1)S_n(y,1)W_n(x,y,z)+zS_n(z,1)W_n(x,z,1)W_n(y,1,1)+z^2S_n(z,1)S_n(z,y)W_n(x,z,1)\\
&+yzS_n(z,1)S_n(y,z)W_n(x,y,1)+zS_n(z,1)W_n(x,1,1)W_n(y,z,1)+S_n(1,y)W_n(x,1,1)W_n(z,1,1)\\
&\left.+yS_n(y,1)W_n(x,1,1)W_n(y,z,1)+yS_n(y,1)W_n(x,y,1)W_n(z,1,1)+W_n(x,1,1)W_n(y,1,1)W_n(z,1,1)\right\}
\end{aligned}
$$

We note that $T_{n+1}(x)$ depends only on the variables $S_n(x,x), S_n(x,1), S_n(1,x), W_n(x,x,x), W_n(x,x,1)$ and $W_n(x,1,1)$. Therefore $T_n(x)$ can be found [62] by solving the following recursive non-linear system of equations for these variables refered in the text as Eq. (46),

$$
\begin{aligned}
T_{n+1}(x) \;=\; & p\,\big\{ x^3 T_n^3(x) + 9x^2 T_n^2(x) S_n(x,x) + 3x^3 T_n^2(x) W(x,x,x) + 24x^3 T_n(x) S_n^2(x,x) + 3x^2 T_n(x) S_n^2(x,1) \\
& + 12x^3 T_n(x) S_n(x,x) W_n(x,x,x) + 6x^2 T_n(x) S_n(x,1) W_n(x,x,1) + 3x^2 T_n(x) W_n^2(x,x,1) \\
& + 14x^3 S_n^3(x,x) + 9x^2 S_n(x,x) S_n^2(x,1) + S_n^3(1,x) \\
& + 3x S_n^2(x,1) S_n(1,x) + 3 S_n^2(1,x) W_n(x,1,1) + 6x S_n(x,1) S_n(1,x) W_n(x,x,1) \\
& + 12x^2 S_n(x,1) S_n(x,x) W_n(x,x,1) + 3x S_n^2(x,1) W(x,1,1) \\
& + 3x^2 S_n^2(x,1) W(x,x,x) + 3 S_n(1,x) W_n^2(x,1,1) + 6 S_n(x,1) W_n(x,1,1) W_n(x,x,1) + W_n^3(x,1,1) \big\} \\[4pt]
S_n(x,x) \;=\; & (1-p)\,\big\{ 2x^2 T_n(x) S_n(x,1) W_n(x,x,1) + x^3 T_n^2(x) S_n(x,x) + 7x^3 T_n(x) S_n^2(x,x) \\
& + x S_n^2(x,1) W_n(x,1,1) + 3x^2 S_n^2(x,1) S_n(x,x) + x S_n(1,x) S_n^2(x,1) + x^3 T_n^2(x) W_n(x,x,x) \big\} \\[4pt]
S_n(x,1) \;=\; & (1-p)\,\big\{ 2x^2 T_n(x) S_n(x,1) W_n(x,1,1) + x^3 T_n^2(x) S_n(x,1) + 4x^3 T_n(x) S_n(x,1) S_n(x,x) \\
& + 2x^2 T_n(x) S_n(1,x) S_n(x,1) + x T_n(1) S_n^2(x,1) + x W_n(1,1,1) S_n^2(x,1) + x^2 S_n^3(x,1) \\
& + 3x S_n(1,1) S_n^2(x,1) + x^3 T_n^2(x) W_n(x,x,1) \big\} \\[4pt]
S_n(1,x) \;=\; & (1-p)\,\big\{ 2 T_n(1) S_n(1,1) W_n(1,x,1) + x^2 T_n(x) S_n^2(1,x) + 4 T_n(1) S_n(1,1) S_n(1,x) + T_n^2(1) S_n(1,x) + \\
& 2x T_n(1) S_n(1,x) S_n(x,1) + S_n^2(1,1) W_n(x,1,1) + 2 S_n^2(1,1) S_n(1,x) + 2x S_n(1,1) S_n(1,x) S_n(x,1) \\
& + T_n^2(1) W_n(1,1,x) \big\} \\[4pt]
W_n(x,x,x) \;=\; & (1-p)\,\big\{ 12x^3 T_n(x) S_n(x,x) W_n(x,x,x) + 3x^3 T_n(x) S_n^2(x,x) + 11x^2 S_n(x,1) S_n(x,x) W_n(x,x,1) \\
& + 4x^2 S_n^2(x,1) W_n(x,x,x) + 6x S_n(1,x) S_n(x,1) W_n(x,x,1) + 6x S_n(x,1) W_n(x,1,1) W_n(x,x,1) \\
& + 3 S_n(1,x) W_n^2(x,1,1) + 3 S_n^2(1,x) W_n(x,1,1) + 14x^3 S_n^3(x,x) + S_n^3(1,x) + 3x^2 T_n(x) W_n^2(x,x,1) \\
& + W_n^3(x,1,1) \big\} \\[4pt]
W_n(x,x,1) \;=\; & (1-p)\,\big\{ 4x^3 T_n(x) S_n(x,x) W_n(x,x,1) + 2x^3 T_n(x) S_n(x,1) W_n(x,x,x) + 2x^2 T_n(x) S_n(1,x) W_n(x,x,1) \\
& + 2x T_n(1) S_n(x,1) W_n(x,x,1) + 2 T_n(1) S_n(1,x) W_n(x,1,1) + 2x^3 T_n(x) S_n(x,1) S_n(x,x) \\
& + T_n(1) S_n^2(1,x) + 3x^2 S_n(x,1) S_n(x,x) W_n(x,1,1) + 3x^2 S_n^2(x,1) W_n(x,x,1) \\
& + x^2 S_n(x,1) S_n(x,x) W_n(x,x,1) + 2x S_n(x,1) W_n^2(x,1,1) + 4x S_n(1,x) S_n(x,1) W_n(x,1,1) \\
& + 6x S_n(1,1) S_n(x,1) W_n(x,x,1) + 2x W_n(1,1,1) S_n(x,1) W_n(x,x,1) + 3 S_n(1,1) W_n^2(x,1,1) \\
& + W_n(1,1,1) S_n^2(1,x) + 6 S_n(1,1) S_n(1,x) W_n(x,1,1) + 2 W_n(1,1,1) S_n(1,x) W_n(x,1,1) \\
& + 6x^3 S_n(x,1) S_n^2(x,x) + 4x^2 S_n(1,x) S_n(x,1) S_n(x,x) + 2x S_n^2(1,x) S_n(x,1) \\
& + 3 S_n(1,1) S_n^2(1,x) + 2x^2 T_n(x) W_n(x,1,1) W_n(x,x,1) + T_n(1) W_n^2(x,1,1) + \\
& W_n(1,1,1) W_n^2(x,1,1) \big\} \\[4pt]
W_n(x,1,1) \;=\; & (1-p)\,\big\{ 2x^3 T_n(x) S_n(x,1) W_n(x,x,1) + 2x^2 T_n(x) S_n(1,x) W_n(x,1,1) + 2x T_n(1) S_n(x,1) W_n(x,1,1) \\
& + 2 T_n(1) W_n(1,1,1) S_n(1,x) + 4 T_n(1) S_n(1,1) W_n(x,1,1) + x^3 T_n(x) S_n^2(x,1) \\
& + 2 T_n(1) S_n(1,1) S_n(1,x) + x^2 S_n^2(x,1) W_n(x,1,1) + x^2 S_n(x,1) S_n(x,x) W_n(x,1,1) \\
& + x W_n(1,1,1) S_n(1,x) S_n(x,1) + 7x S_n(1,1) S_n(x,1) W_n(x,1,1) + 2x W_n(1,1,1) S_n(x,1) W_n(x,1,1) \\
& + W_n^2(1,1,1) S_n(1,x) + 6 S_n(1,1) W_n(1,1,1) S_n(1,x) + 8 S_n^2(1,1) W_n(x,1,1) \\
& + 6 S_n(1,1) W_n(1,1,1) W_n(x,1,1) + 2x^3 S_n^2(x,1) S_n(x,x) + 2x^2 S_n(1,x) S_n^2(x,1) \\
& + 4x S_n(1,1) S_n(1,x) S_n(x,1) + 7 S_n^2(1,1) S_n(1,x) + x^2 T_n(x) W_n^2(x,1,1) \\
& + 2 T_n(1) W_n(1,1,1) W_n(x,1,1) + W_n^2(1,1,1) W_n(x,1,1) \big\} \qquad (83)
\end{aligned}
$$